Platinum vaporization-deposition coated polycarbonate membranes for comprehensive, multimodal, and correlative microscopic analysis of

Talanta 269 (2024) 125435

Contents lists available at ScienceDirect

Talanta

journal homepage: www.elsevier.com/locate/talanta

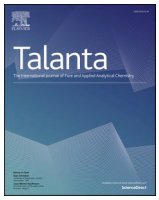

Platinum vaporization-deposition coated polycarbonate membranes for comprehensive, multimodal, and correlative microscopic analysis of micro-and nanoplastics and other environmental particles

Karin Mattsson [a,*], Mats Hagberg [b], Martin Hassellöv [a]

[a] Department of Marine Sciences, University of Gothenburg, Kristineberg Marine Research Station, SE-451 78 Fiskebäckskil, Sweden
[b] Department of Microtechnology and Nanoscience, Chalmers University of Technology, Gothenburg, Sweden

ARTICLE INFO

Keywords:
Membranes
Polycarbonate
Microplastics
Analytical techniques
Spectroscopy

ABSTRACT

Anthropogenic particles, including microplastics, are receiving ever-increasing concern due to their potential environmental impact. Surveys and monitoring require sampling from many environmental and biological matrices, including natural water, drinking water, sediment, and air. However, there are no standard methods for sampling particles in the environment; thereby, many different approaches are used for both single particle and ensemble distribution or bulk chemical analyses. In the microplastics field, particles are often analyzed on membranes using automated analysis with spectroscopic techniques such as Fourier-transform infrared spectroscopy (FTIR) and Raman spectroscopy. For automated analysis, the filters' properties are crucial. We coated polycarbonate (PC) membranes with 100 nm platinum (Pt) on both side using a e-beam evaporator and evaluated their suitability for filtrating and analysis of environmental samples. The PC membranes have a defined and practical pore size, available in many pore sizes and with circular diameter of 47 mm and 25 mm. Our Pt coated membranes can handle large volumes of fresh and marine waters, high pressure, and various treatment solutions. Moreover, they have good optical properties for imaging with light microscopy (LM) and Scanning Electron Microscopy (SEM), and no disturbing background signal for Raman or FTIR spectroscopy analysis.

1. Introduction

Anthropogenic particles, including microplastics [1], are sampled from biological, technical and environmental matrices, such as water, sediment, and air. For example, in the marine environment, anthropogenic particles are sampled from surface water [2], the pelagic water column, sediments [3], and biota [4]. However, there are no standard methods for sampling particles in the environment [5–8]; therefore, many different approaches are used for both single particle and ensemble distribution or bulk chemical analyses. Most widely used technique for single particle analysis is microscopy-based techniques such as Raman microscopy and Fourier-transform infrared spectroscopy (FTIR), and for bulk analysis it is pyrolysis-gas-chromatography-mass spectroscopy (py-GCMS) [9].

Analytical filtration for microscopy particle analysis, single particle count, and characterization have specific prerequisites and demands on the filtration setup and filters. These derive from particle filtration process behavior, the filter integrity, its properties, and the requirements of subsequent analysis with different modes of microscopy.

The membrane should have well-defined pore size distribution, and particle selection should occur on the filters' surface rather than depth filtration, which occurs in many common membrane types. The porosity or pore coverage should be high to avoid clogging from occurring prematurely. Clogging of pores with both analyte and background particles will unenviably occur at some point during the filtration of a sample. It is known that filter pore size distribution and, thus, adequate particle selectivity change much before clogging, leading to pressure buildup [10,11]. In order to increase the clogging volume for a given filter, a cascade filtration setup with a sequential series of filters with a stepwise smaller pore size can be used. However, it should be noted that the retention of particles defines the nominal pore size cutoff and not the free-passing particle size, this previous filter will influence the next, and holistic analysis is needed.

For microplastics, the most commonly used sampling techniques are bulk sampling, i.e., the entire sample volume is collected and not reduced during the sampling, or volume-reduced sampling, i.e., the

* Corresponding author.
E-mail address: Karin.mattsson@gu.se (K. Mattsson).

https://doi.org/10.1016/j.talanta.2023.125435
Received 29 August 2023; Received in revised form 23 October 2023; Accepted 17 November 2023
Available online 22 November 2023

Abbreviations

BF	Bright Field
DF	Dark Field
EDX	Energy dispersive X-ray spectroscopy
FTIR	Fourier Transform Infrared
H_2O_2	Hydrogen peroxide
LM	Light Microscopy
PC	Polycarbonate
PS	Polystyrene
Pt	Platinum
PVP	Polyvinylpyrrolidone
Py-GCMS	Pyrolysis-gas chromatography-mass spectroscopy
SEM	Scanning Electron Microscopy
$ZnCl_2$	Zinc Chloride

sample is reduced while collected, such as through filtration [8]. In both cases, the particles of interest will end up on filters. Often, a chemical or enzymatic treatment is applied to the samples to reduce organic matter [12]. This can be either before the particles reach the filters, when they are on the filters, or both. The filters are then analyzed visually and spectroscopically [8]. To avoid contamination from the surroundings [13], as little sample and filter handling are desired, direct analysis of the particle on the filters is preferable. Typically, visual identification occurs through a light microscope (LM), where the particles are measured and characterized according to their visual appearance [8, 14]. Then, the spectroscopic identification takes place, generally with FTIR or Raman spectroscopy, to identify the specific polymer. For particles larger than 300 μm, the structure of the filters is less crucial as for smaller-sized particles, basically due to magnification and comparably less interaction with the background. The size distribution of particles collected in the environment shows a higher abundance of particles within the smaller-sized classes [15–17]. Because of their small size, high abundance of particles, and a potential biased impact from the operator [8,18–20], automated analysis is required. For automated analysis, the filters' surface has to be unstructured and smooth and have good optical contrast, low Raman, and fluorescence signal, especially in the range of polymer bands. If Scanning Electron Microscopy (SEM) analysis is desired, the filter's and particles' conductivity is essential, especially under high vacuum conditions. The filters should also not be affected by high pressure from the filtration, treatments to reduce organic matter, and have a defined pore size and pore distributions and not be fragile. Preferably many filters made of the same material but with different pore sizes can be used during the sampling of particles. Subsequently, the filters would be put through the analysis pipeline with one or another mode of micro-spectroscopy or even correlative microscopy workflows. The filtration process needs to be more carefully considered and optimized for smaller pore sizes when diffusion of small-sized particles plays a more prominent role than simple sieving, slow filtration rate, and large porosity and cascade filtration are important considerations [21,22].

There are many available filters on the market, with different strengths and limitations, both from the filtration properties such as accuracy and reproducibility of pore size, porosity and clogging propensity, sorption or contamination of analyzed, and suitability for different types of microspectroscopic analysis. These include silicon wafer filters, aluminum oxide (Anodisc, Whatman) and different polymer-based membranes like track edged polycarbonate (PC) (several different manufactures available). Aluminum oxide filters are only available in 47 mm, 25 mm, and 13 mm sizes, with two pore sizes, 200 nm, and 20 nm. They can be used with both FTIR (transmission mode) and Raman; they are smooth but have a pattern on their surface, impacting the visual analysis with LM and SEM, especially if the particles of interest are white, transparent, or semi-transparent. The track-etched PC membrane filters are commercially available in different diameters and pore sizes. However, since PC is an analyte polymer, it is not practical to use for spectroscopic identifications since the background signal from the filter can interfere with the actual signal from the particles of interest. It is even more complicated if the particles are polycarbonate. Gold-coated PC membranes have good optical properties in the darkfield but give a weak fluorescence Raman signal from the background [23]. When evaluating gold-coated filters with polystyrene (PS) reference particles, the intensity of the Raman background signal from the membrane interfered too much with the signal from the PS particles.

Table 1
Membrane specifications.

Pore size	30 μm	10 μm	1 μm	0.4 μm
Thickness	30 μm	10 μm	11 μm	10 μm
Hydrophilic/ Hydrophobic	Hydrophilic	Hydrophobic	Hydrophobic	Hydrophobic
PVP-free	No	Yes	Yes	Yes
Diameter	47 mm	47 mm	25 mm	25 mm
Pore size before coating	28.17 ± 0.26 μm	10.01 ± 0.24 μm	0.94 ± 0.06 μm	0.34 ± 0.02 μm
Pore size after coating	27.89 ± 0.28 μm	10.31 ± 0.18 μm	1.03 ± 0.03 μm	0.49 ± 0.02 μm

Using electron beam evaporation, PC filters have been coated with titan, nickel, and aluminum. The membranes coated with titan or nickel have been shown to have similar optical properties as gold-coated membranes and no signal from the PC background. However, with titan, it was not possible to obtain a Raman signal from the PS reference particles with a 532 nm laser, and with nickel, it was not possible to acquire a Raman signal with a 785 nm laser [23]. On the other hand, aluminum-coated PC membranes had mirror properties and showed good optical performance in both bright field (BF) and dark field (DF). However, in BF it is challenging to automatically distinguish between holes and particles. In addition, there was no signal from the background, only a weak fluorescence signal with a 785 nm laser; however, the Raman intensity was much higher than for gold-coated membranes.

We aimed to develop filters made of one type of material with a defined and practical pore distribution, available in many pore sizes and with a circular diameter of 47 mm and 25 mm. Moreover, the membranes must be able to handle high pressure, filtrate a large volume of solutions, withstand chemical or enzymatic treatments, low background signal from filters that do not interfere with the polymeric fingerprint, as well as good properties in SEM with various detectors and performing well in different imaging modes of LM. The SEM criteria include good charge dissipation, and ideally as low or as high atomic number as possible so the sample material that typically distributes from carbon to copper, would have different contrast in backscattering detectors.

2. Material and methods

2.1. Membrane selection

Filters fulfilled purpose criteria: a smooth and unstructured surface, defined pore sizes, pore distribution, not brittle or fragile, available in two circular diameters (47 mm and 25 mm), and many different pore sizes were track edge PC membranes supplied from Sterlitech (Auburn, WA, USA). Only hydrophilic membranes are available for membranes with a pore size of 30 μm; however, for 10, 1, and 0.4 μm, both hydrophilic and hydrophobic, as well as free from PVP (polyvinylpyrrolidone) exist. Membrane specifications presented in Table 1.

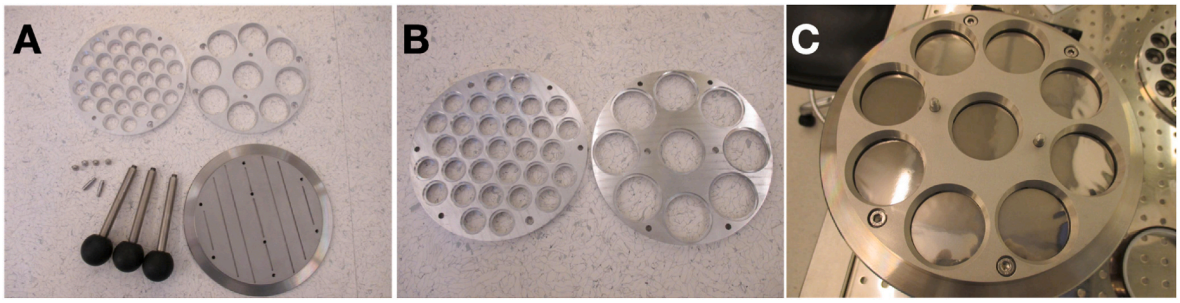

Fig. 1. A-B) Membrane holders for 47 mm and 25 mm filters and C) Platinum coated filters in a holder.

2.2. Magnetron sputtering

A load-locked magnetron sputter system configured sputter-down, i.e., the sputter target located 7 cm above the substrate tray. In this configuration, the objects to be coated can often be kept in place by gravity only. A few filter membranes were placed on the substrate tray, with the shiny side up and weight clamped with metal rings, and 100 nm aluminum was deposed with argon plasma.

2.3. E-beam evaporation

For evaporation with an e-beam evaporator, a load-locked system built by Kurt J. Lesker Company was used. It has a substrate tray located 49 cm above the crucible. For the initial test, filter membranes with 47 and 25 mm diameters and 30, 10, 1, and 0.4 μm pore sizes were attached to three 150 mm silicon wafers using three or four small strips of Kapton tape per membrane. The silicon wafers were attached to the substrate tray, and the filter membranes were single-sided coated with 100 nm aluminum or 100 nm platinum (Pt) at a rate of 3 Å/s.

2.4. Membrane holder plates

In order to keep the filter membranes stretched flat during the deposition process, two 8 mm thick aluminum plates were fabricated. The top plate had openings slightly smaller than the membranes. A nitrile rubber o-ring was placed in a recess around each hole to increase friction and ensure uniform pressure when this aluminum plate was used to clamp the membranes against the substrate plate. The openings were fabricated for the back side plate without recess around the holes (Fig. 1).

2.5. Test samples

Tap water from different locations in Sweden was filtrated in a cascade filtration setup with 100, 30, 10, 1, and 0.4 μm membranes. The 10 and 1 μm membranes were coated with aluminum. For the 10 μm membranes, volumes between 200 and 400 L were filtrated, and for the 1 μm filters, 0.5–3 L were filtrated.

Different anthropogenic particles, including black particles, paint particles, fibers, and plastic particles collected from the environment and some reference plastic particles, were transferred using tweezers to a Pt-coated membrane and analyzed with LM, Raman spectroscopy, and SEM.

Cryo-milled PS particles were transferred with a tweezer to a Pt-coated membrane and imaged, and spectra were obtained with Raman microscopy from the particles and the background. As a comparison, PS particles were transferred with a tweezer to an uncoated PC membrane and imaged and analyzed with Raman microscopy.

Pieces of beach litter was collected and filed into micro-sized particles, which were placed on a Pt-coated membrane and analyzed with Raman microscopy and FTIR in transmission mode using a cooled detector.

To include biological samples, a planktonic trawl (mesh size 90 μm) from 25 m of depth was collected in the Gullmarn fjord, filtered on a Pt-coated membrane, and imaged with SEM.

2.5.1. On-filter sample preparation treatments

Water samples (marine water and tap water) were treated directly after filtration in their cascade filtration setup with 10 % filtrated (0.4 μm) hydrogen peroxide (H_2O_2). Sediment samples were treated with a chemical treatment [24], then separated with Zinc Chloride ($ZnCl_2$) and filtrated through the membranes. Fish tissue was treated with enzymes [25], then filtrated through membranes. However, the membranes were also exposed directly to different commonly used solutions for organic matter degradation including enzymes (Tris-Creon) [25], two chemical treatments [24,26], and, H_2O_2. Moreover, the membranes were exposed to and an acid treatment (20 % of hydrofluoric acid (48–50 %) and 10 % hydrochloric acid (37 %)) in room temperature during 3 h for dissolution of minerals.

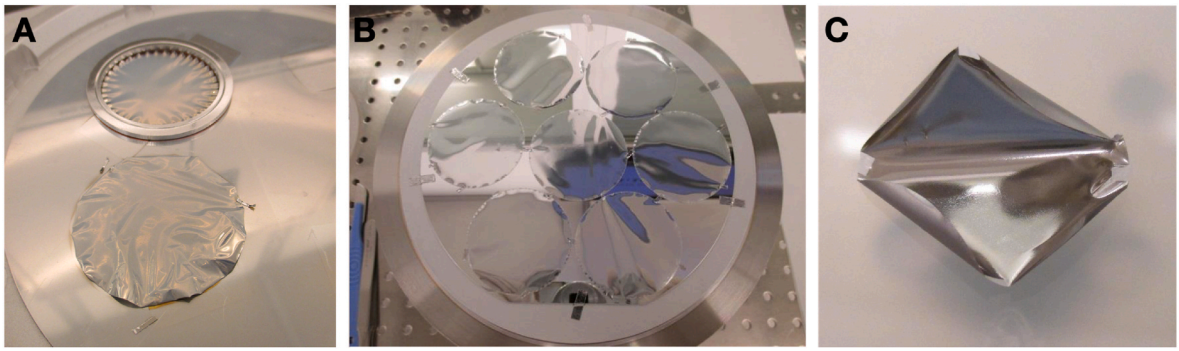

Fig. 2. Membranes after A) Sputtering with aluminum B) Evaporation with aluminum and C) Evaporation with platinum on one side of the membrane.

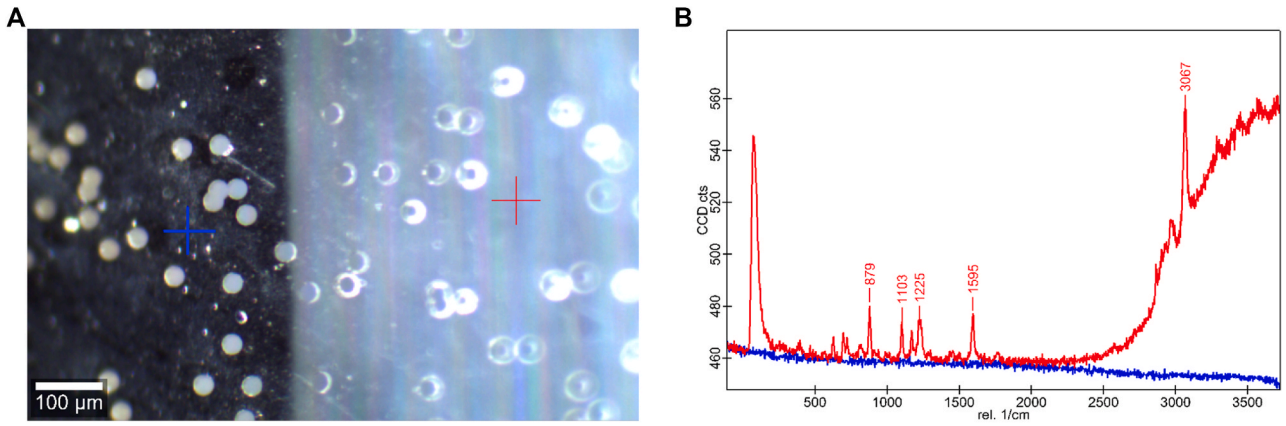

Fig. 3. A) Image of the 30 µm membrane where one part has been coated (left) and one remained uncoated (right) and B) Raman spectra of the coated part of membrane (blue) and uncoated PC membrane (red). Spectra obtained using 10x objective, 10 accumulations with 0.5 s of integration time. Spectra are not baseline corrected.

2.6. Imaging and spectroscopic analysis (LM, SEM, Raman, FTIR)

Light microscopy imaging was performed with a Zeiss Axio Imager equipped with 5x, 10x, 20x and 50x objectives with possibility to image both in DF and BF. Entire membranes (47 mm diameter) with z-stacking can be imaged. SEM images were obtained on a Zeiss Gemini 300 and a SEM Zeiss Sigma VP both equipped with a backscatter detector, secondary electron detector, in-lens SE detector and a Bruker energy dispersive X-ray spectrometer (EDX). Raman microscopy analyses were performed on a WiTec Alpha 300 R microscope equipped with a 532 nm laser and 600 g/mm grating. Imaging can be performed in both BF and DF with 5x, 10x, 20x, and 50x objectives. Laser power depending of the size of analyzed particles and in general 10–50 accumulations for 0.5 s were recorded. FTIR was performed on a Thermo Scientific Nicolet iN10 infrared microscope equipped with a cooled detector. Measurements were performed in reflectance mode, 128 scans and a background obtained directly after the spectra with a wavenumber range of 4000-675 cm^{-1}.

3. Results and discussion

3.1. Sputtering vs. evaporation

Aluminum with a thickness of 100 nm was metalized on the PC membranes with sputtering. After the deposition of aluminum with argon plasma, the membranes were severely deformed (Fig. 2A). It is probably due to that the argon plasma radiation overheated the PC membranes. The mechanical properties of the very thin membranes make them virtually impossible to heat-sink. Therefore, no more magnetron sputtering attempts were made.

With the e-beam evaporator, 100 nm of aluminum was applied to the PC membranes' shiny side, resulting in flat membranes with mirror-like surfaces (Fig. 2B). On the other hand, evaporating 100 nm, Pt on the shiny side of the PC membranes resulted in curled membranes towards the coated face and instantly rolled up into cylinders when detached from the silicon wafer (Fig. 2C). These cylinders are very difficult to handle, loading them in the filter holders and after filtration for the analysis process. This much different result can be explained by the substantially higher temperature of the radiating platinum source and platinum's mechanical hardness. Both properties can induce higher tensile stress in the membranes. In order to keep the filter membranes stretched flat during the deposition process, we fabricated the filter holding plates (Fig. 1), in order to be able to coat them on both sides.

Membranes coated on both sides with 100 nm Pt resulted in flat filters when first coating the shiny side and then the backside is shown in Fig. 1. However, when the rough side were first coated the membranes rolled up and formed cylinders. It is possible that flat membranes could also be obtained if the rough (back) side would be coated with a different metal. However, this would require more process development in order to find suitable metallic material and thickness. This particular metal would also have to withstand the chemicals or enzymes used to reduce organic matter.

3.1.1. Aluminum coating integrity

The aluminum coated filters had good optical properties in LM, no interference from the background with Raman spectroscopy, and good properties for SEM (charge dissipation and low atomic number). These filters were used for filtrating tap water. Volumes between 200 and 400

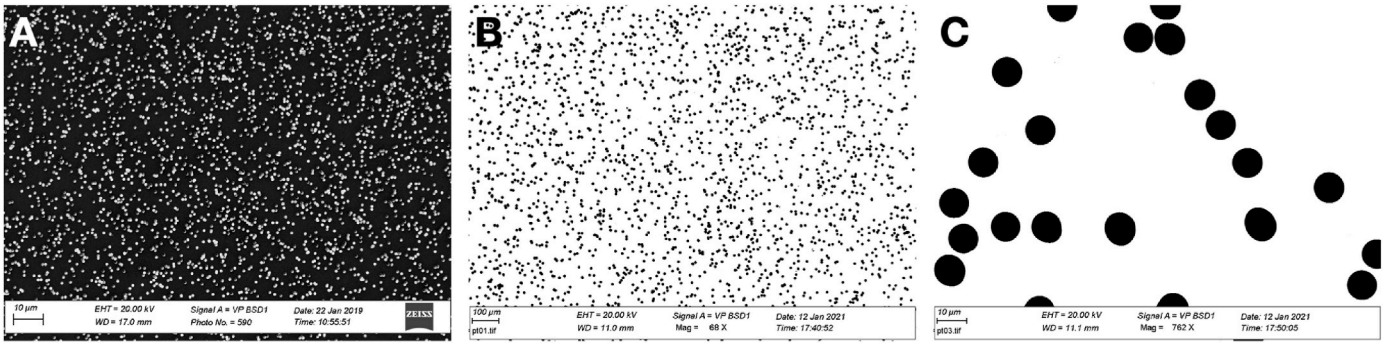

Fig. 4. Membranes imaged with SEM in VP mode, 20 kV and using the backscatter detector A) Al coated 1 µm membranes and B–C) Pt-coated membranes, with a pore size of 10 µm, imaged with SEM using typical settings for automated analysis using SmartPI and SEM-EDX measurements [27], and different magnifications B) 68× and C) 762 X.

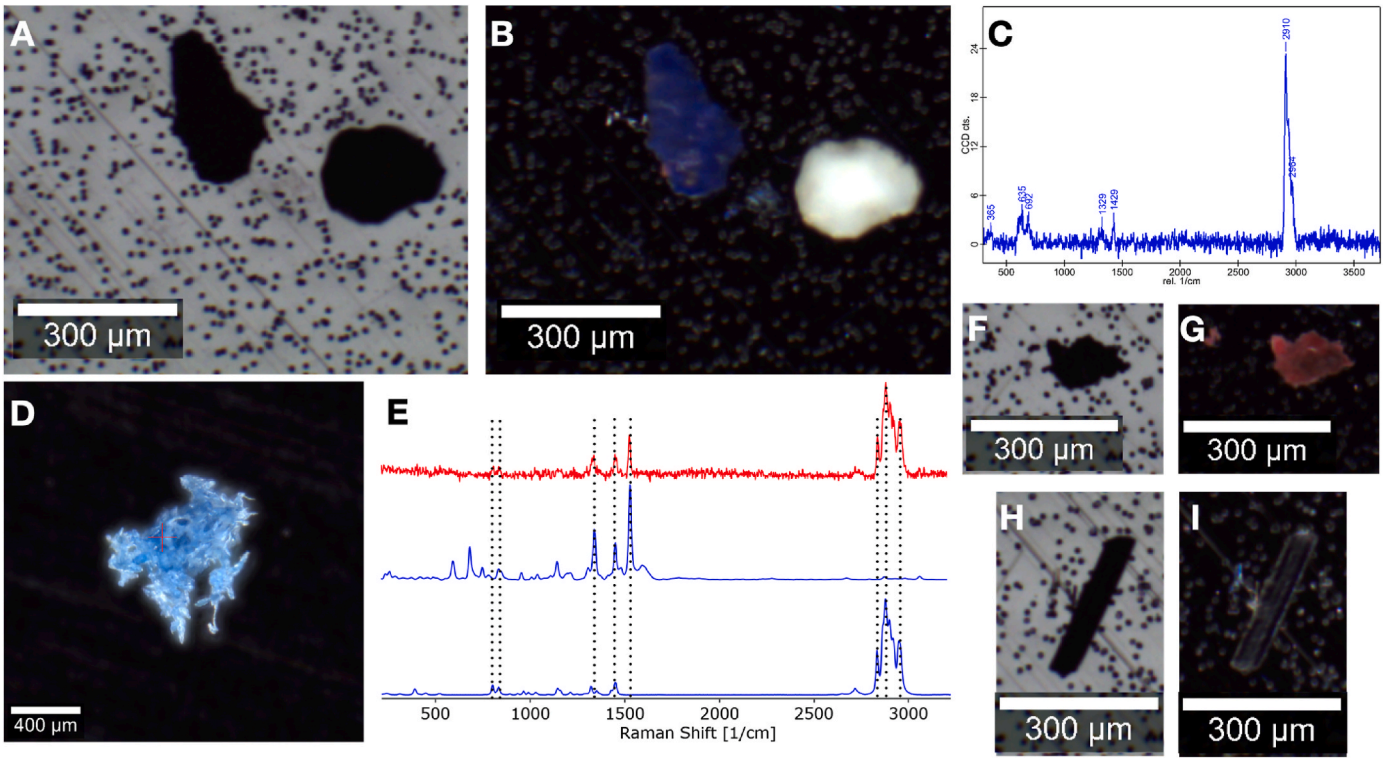

Fig. 5. A-B) Raman microscopy images in DF and BF using a 5x objective of a paint particle and a PVC particle collected in the environment and C) Raman spectra of PVC particle in A-B. D) DF image of a blue PP particle collected on a beach and filed into micro-sized, E) Raman spectra of particle D (red) with reference spectra for blue color (top blue) and PP (lower blue). DF and BF image of F-G) red plastic particles, and H–I) black fiber.

L were filtered through 10 µm membranes with pressure up to 2 bars. For 1 µm membranes, between 0.5 and 3 L were filtered with a pressure of up to 0.2 bar. In most cases, for the 10 µm membranes, the coating was damaged. However, for the 1 µm, most membrane coatings were intact, implying that the aluminum coating cannot handle high pressure and/or filtering of large volumes. This was in contrast to the findings by Ossmann et al., 2017 that recommended aluminum coated filters, however in that study only a small volume (250 mL) of sample was passed through the filters. Aluminum deposited in the vacuum may not have a protective oxide layer, and 100 nm aluminum could be significantly oxidatively destroyed by passing large volumes of water and in contact with water during several hours. Additionally, the integrity of the thin aluminum coating would be susceptible to further damage as a results of any post-filtration chemical treatments. The overall conclusions is therefore that aluminum is not a recommended coating metal to explore further.

3.1.2. *Issues hydrophilic vs. hydrophobic membranes and PVP free*

The hydrophilic non-PVP-free PC membranes showed an increased fluorescence signal with Raman spectroscopy. The 30 µm membranes are unfortunately not available as PVP-free. However, the fluorescent signal disappeared after the coating with 100 nm Pt on both sides (Fig. 3).

3.2. *Platinum coating membranes*

Membranes metalized with 100 nm platinum on both sides using e-beam evaporation and membrane holder plates resulted in mirror-like membranes (Figs. 1 and 4). The pore size of the filters was measured with SEM before and after coating, and there was a slight increase in pore size for 10, 1, and 0.4 µm, while for 30 µm, there was a small decrease after the membranes were coated (Table 1). For identification and characterization of anthropogenic particles with SEM imaging, a clear contrast between particles and background is critical so either the background should have a low atomic number or a high. Moreover, for automated analysis the back scatter detector and EDX measurements are necessary, which puts requirements on working distance and voltage [27].

3.2.1. *Treatments*

Tap water and marine water have been filtrated in a cascade filtration setup and directly treated with 10–30 % H_2O_2, without damaging the membranes. To evaluate effects of concentration and/or exposure time, one membrane was exposed to 10 % of H_2O_2 during 10 min, followed by 20 % during 10 min and then 30 % during 10 min. The first three treatments were successful without affecting the surface. However, after 4 treatments small parts of coating came loose. Sediments have been treated with chemicals [24,28] and then separated with $ZnCl_2$ and filtrated through Pt-coated membranes without any surface effects. After filtration the membranes were rinsed with deionized water (Milli-Q) and dried. Fish tissue have been treated with enzymes [25] and after treatment the solution were filtrated through membranes without any interference or damages of the membranes. After filtration the membranes were rinsed with Milli-Q water and dried. Membranes without any particles were exposed to H_2O_2, chemicals [26,28] and enzymes [25] according to the protocol [25,26,28]. The H_2O_2 and chemical solution developed by Strand et al., did not affect the membranes, however, the enzymatic treatment and the chemical treatment developed by Enders et al., resulted in damaged surfaces. Tire and road wear particles were treated with an acid treatment (20 % solution of concentrated hydrofluoric acid (48–50 %) and 10 % solution of concentrated hydrochloric acid (37 %)) to remove minerals incrusted in the particles. The particles were treated on the membranes in room temperature for 3 h and after treatment the filters were rinsed with Milli-Q and the particles and the membranes surface were analyzed with SEM where the membranes still were intact without any artifacts in the coating.

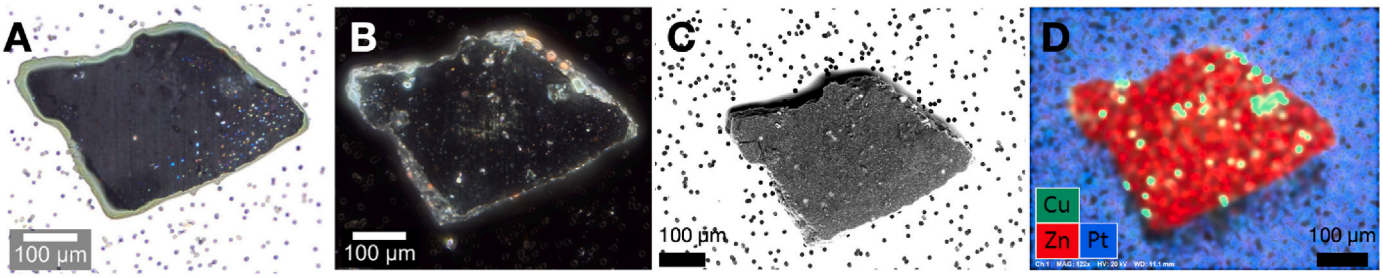

Fig. 6. Paint particle imaged with A) BF using Raman microscopy, 20x objective and focus stacking, B) DF using Raman microscopy, 20× objective and focus stacking C) SEM using the Back Scatter detector in VP mode and 20 kV, and D) SEM-EDX mapping of zinc, copper, and platina.

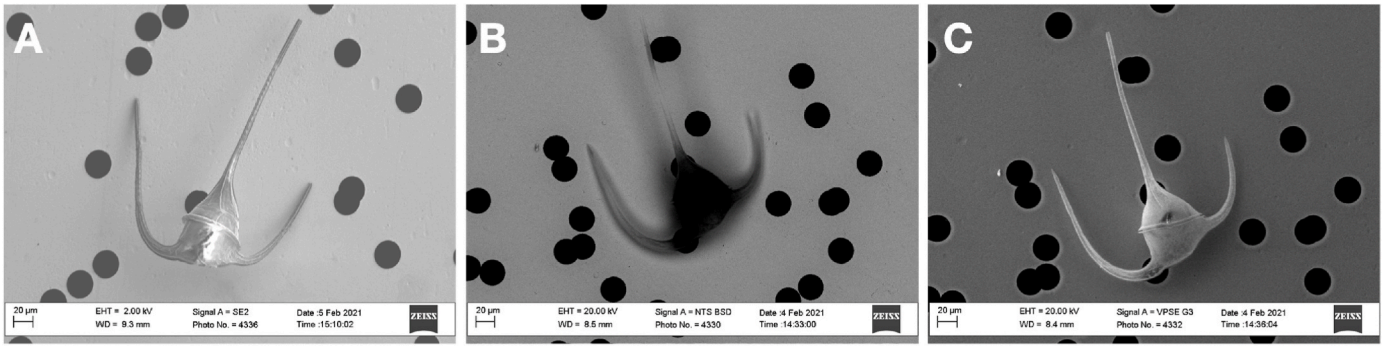

Fig. 7. SEM images of Dinoflagellates imaged with A) secondary electrons, B) backscatter detector, and C) secondary electrons in variable pressure.

Table 2
Vibration modes for PC, PVC, PS and PE.

PC		PVC		PS		PE	
cm^{-1}	vibration mode	cm^{-1}	vibration mode	cm^{-1}	vibration mode	cm^{-1}	vibration mode
879	O-C(O)-O stretching	361	C-Cl bending	614	ring deformation mode	720	CH_2 rock
1103	C-O-C stretching	636	C-Cl in Cl2C=CHCl stretching	795	C-H out of plane deformation	1376	CH_3 bending
1225	C-O-C stretching	695	C-Cl in H2C=CHCl symmetric stretching	1001	ring breathing mode	1474	CH_2 bending
1595	phenyl ring vibration	1329	CH bending	1031	C-H in plane deformation	2846	C-H symmetric stratch in CH_2
3067	C-H stretching	1429	CH_2 bending	1150-1200	C-C stretch	2914	C-H asymmetric stretch in CH_2
		2910	C-H stretching in -CH_2 structure	1450	CH_2 scissoring		
				1583	C=C stretch		
				1602	ring skeletal stretch		
				3000	C-H vibrations		

3.2.2. *Light and electronic microscopy properties*

A sample containing black particles, paint particles, fibers, and plastic particles from the environment and reference plastic particles were imaged in Raman microscopy with bright field (BF) and dark field (DF) (Fig. 5 and Fig. S1), and in s SEM using different detection modes. When imaged with BF, all particles were visible; however, it was more challenging with particles close to the pore size to distinguish between particles and holes. In DF, all particles were visible; however, the black particles were more difficult to see. There were no problems distinguishing particles from holes. For automated image analysis in BF,

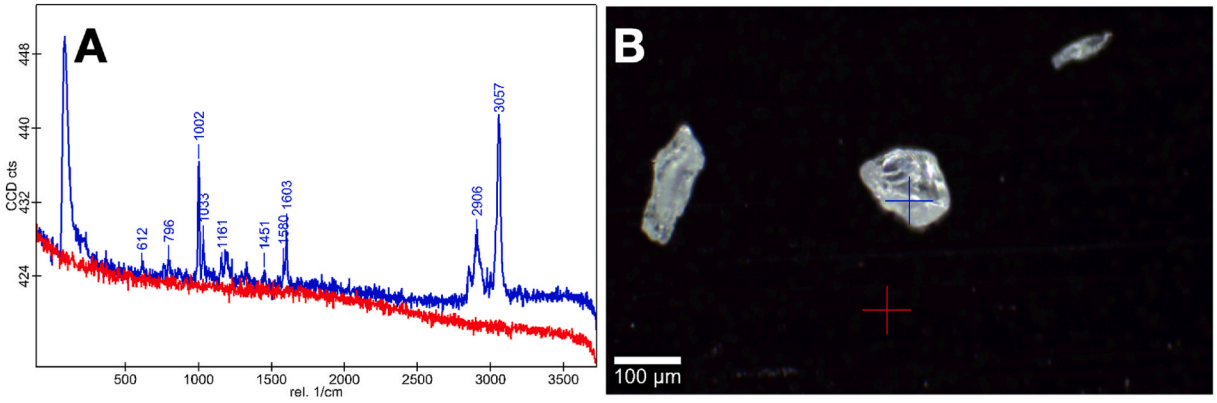

Fig. 8. A) Raman spectra of a PS particle (blue), background spectra (red), and B) image of the particle with marks where spectra were obtained. Laser power 1.5 mW, 600 g/mm grating, 10x objective, 50 accumulations and 0.5 s integration time.

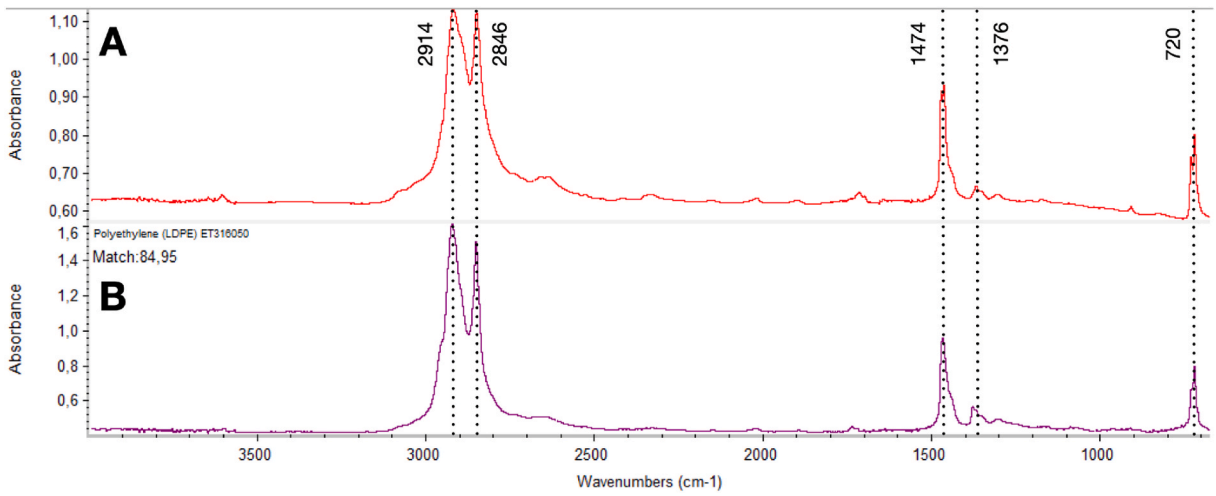

Fig. 9. FTIR spectra obtained with reflectance mode, 128 scans with a background collected directly after the particle spectra of A) field beach micro-litter and B) reference PE spectra.

there were no problems. At the same time, in DF, the dark particles had to be identified separately from the lighter ones, i.e., the light particles can be automatically identified, then the dark or the other way around. The same sample were also analyzed with SEM and EDX with excellent performance (Fig. 6).

Dinoflagellates were filtered on a Pt-coated membrane and imaged with SEM in high vacuum and in variable pressure (Fig. 7). To be able to image organic, insulator specimens in high vacuum without sputtering with a conductive material such as gold or carbon, is a great advantage in imaging size resolution. In the SE2 detector in high vacuum (Fig. 7A) there is possibly a small charge buildup on some edges, on the diatoms but very little, and the resolution was better than the variable pressure secondary electron detector (Fig. 7B).

3.2.3. Spectroscopic properties

The Pt-coated membrane itself, as well as the PVC particle in Fig. 5A and B (white), were analyzed with Raman spectroscopy (Fig. 5C). From the particle, precise PVC spectra were obtained, with characteristics peaks for PVC (Table 2), with no interference from the background, and from the Pt coating, no disturbing signals were obtained. PS particles were also analyzed with Raman microscopy, and precise spectra of PS were obtained, with characteristic peaks for PS (Table 2), with no interference from the background (Fig. 8). High hit rates were obtained on Pt-coated and uncoated membranes for larger-sized particles, i.e., particles larger than the laser spot. However, when measuring particles smaller than the laser spot, interference from the uncoated membranes was clear, with 62 % PS match and 38 % PC match, while for Pt-coated membranes, the hit rate was 93 % for PS (Fig. S2).

The North Sea beach micro-litter particle was analyzed with Raman microscopy (Fig. 5D and E) and FTIR on the Pt-coated membranes without any interference from the background or problems in identifying the blue polypropylene particles (Fig. 5E) and polyethylene particles (Fig. 9).

4. Conclusions

PC coated membranes with 100 nm Pt on both sides resulted in flat mirror like membranes. The membranes can handle large volumes of fresh and marine waters, high pressure, and various treatment solutions for water samples. They also have good optical properties and can be used both in DF and BF, however, with BF, particles with a size close to the pore-size of the membranes, automated identification is limited due to the challenge to distinguish particles from holes. In DF, particles are clearly visible and no interference from the holes in the membranes, however, two thresholds had to be applied to automatically select particles to analyze, i.e., one for the dark/black particles and one for the others. Since Pt has a high atomic number, the SEM properties are good, where anthropogenic particles easily can be imaged with automated analysis with SmartPI for example. For spectroscopic analysis with Raman and FTIR spectroscopy there were no disturbing signal from the background and no fluorescence.

Author Contributions

KM contributed with Conceptualization, Data curation, Formal analysis, Funding acquisition, Investigation, Methodology, Validation, Visualization, Writing – original draft and review & editing. Mats H contributed with Data curation, Formal analysis, Investigation, Methodology, Validation, Visualization and Writing - review & editing. Martin H contributed with Conceptualization, Funding acquisition, Methodology, Visualization and Writing - review & editing. All authors have given approval to the final version of the manuscript.

Declaration of competing interest

The authors declare that they have no known competing financial interests or personal relationships that could have appeared to influence the work reported in this paper.

Data availability

Spectra rawdata will be made available on request.

Acknowledgment

This work was funded by the JPI-Ocean projects ANDROMEDA (grant number 2019-02166 FORMAS) and FACTS (grant number 2019-02169 FORMAS), as well as the Swedish Environmental Protection Agency, SNV. We would also like to thank Linda Svanberg at Kristineberg Marine Research Station for providing Dinoflagellates.

Appendix A. Supplementary data

Supplementary data to this article can be found online at https://doi.org/10.1016/j.talanta.2023.125435.

References

[1] N.B. Hartmann, et al., Are we speaking the same language? Recommendations for a definition and categorization framework for plastic debris, Environ. Sci. Technol. 53 (3) (2019) 1039–1047.

[2] A. Cozar, et al., Plastic debris in the open ocean, Proc. Natl. Acad. Sci. U.S.A. 111 (28) (2014) 10239–10244.

[3] M. Haave, et al., Different stories told by small and large microplastics in sediment - first report of microplastic concentrations in an urban recipient in Norway, Mar. Pollut. Bull. 141 (2019) 501–513.

[4] A.L. Lusher, et al., Microplastic interactions with North Atlantic mesopelagic fish, ICES J. Mar. Sci. 73 (4) (2016) 1214–1225.

[5] A.A. Horton, et al., Microplastics in freshwater and terrestrial environments: evaluating the current understanding to identify the knowledge gaps and future research priorities, Sci. Total Environ. 586 (2017) 127–141.

[6] L. Van Cauwenberghe, et al., Microplastics in sediments: a review of techniques, occurrence and effects, Mar. Environ. Res. 111 (2015) 5–17.

[7] N.P. Ivleva, A.C. Wiesheu, R. Niessner, Microplastic in aquatic ecosystems, Angew. Chem. Int. Ed. 56 (7) (2017) 1720–1739.

[8] V. Hidalgo-Ruz, et al., Microplastics in the marine environment: a review of the methods used for identification and quantification, Environ. Sci. Technol. 46 (6) (2012) 3060–3075.

[9] K. Mattsson, et al., Monitoring anthropogenic particles in the environment: recent developments and remaining challenges at the forefront of analytical methods, Curr. Opin. Colloid Interface Sci. 56 (2021).

[10] A.J. Horowitz, et al., Problems associated with using filtration to define dissolved trace element concentrations in natural water samples, Environ. Sci. Technol. 30 (3) (1996) 954–963.

[11] M.A. Morrison, G. Benoit, Filtration artifacts caused by overloading membrane filters, Environ. Sci. Technol. 35 (18) (2001) 3774–3779.

[12] F. Pfeiffer, E.K. Fischer, Various digestion protocols within microplastic sample processing-evaluating the resistance of different synthetic polymers and the efficiency of biogenic organic matter destruction, Front. Environ. Sci. 8 (2020), 572424.

[13] J.C. Prata, et al., The importance of contamination control in airborne fibers and microplastic sampling: experiences from indoor and outdoor air sampling in Aveiro, Portugal. Mar Pollut Bull 159 (2020), 111522.

[14] T.M. Karlsson, et al., Comparison between manta trawl and in situ pump filtration methods, and guidance for visual identification of microplastics in surface waters, Environ. Sci. Pollut. Res. Int. 27 (5) (2020) 5559–5571.

[15] K. Enders, et al., Abundance, size and polymer composition of marine microplastics >/=10mum in the Atlantic Ocean and their modelled vertical distribution, Mar. Pollut. Bull. 100 (1) (2015) 70–81.

[16] A. Ter Halle, et al., Understanding the fragmentation pattern of marine plastic debris, Environ. Sci. Technol. 50 (11) (2016) 5668–5675.

[17] S. Primpke, et al., An automated approach for microplastics analysis using focal plane array (FPA) FTIR microscopy and image analysis, Anal. Methods 9 (9) (2017) 1499–1511.

[18] R. Lenz, et al., A critical assessment of visual identification of marine microplastic using Raman spectroscopy for analysis improvement, Mar. Pollut. Bull. 100 (1) (2015) 82–91.

[19] M.G.J. Löder, G. Gerdts, Methodology used for the detection and identification of microplastics—a critical appraisal, in: M. Bergmann, L. Gutow, M. Klages (Eds.), Marine Anthropogenic Litter, Springer, Cham., 2015.

[20] K.O. Renner, et al., A comparison of different approaches for characterizing microplastics in selected personal care products, Environ. Toxicol. Chem. (2021).

[21] J. Buffle, J. Perret, J. Newman, The use of filtration and ultrafiltration for size fractionation of aquatic particles, colloids and macromolecules, in: J. Buffle, H. P. van Leeuwen (Eds.), Environmental Particles I, Lewis, Chelsea, 1992.

[22] J. Buffle, G. Leppard, Characterization of aquatic colloids and macromolecules. 1. Structure and behavior of colloidal material. 2. Key role of physical structures on analytical results, Environ. Sci. Technol. 29 (1995) 2169–2184.

[23] B.E. Ossmann, et al., Development of an optimal filter substrate for the identification of small microplastic particles in food by micro-Raman spectroscopy, Anal. Bioanal. Chem. 409 (16) (2017) 4099–4109.

[24] K. Mattsson, et al., Comparison of pre-treatment methods and heavy density liquids to optimize microplastic extraction from natural marine sediments, Sci. Rep. 12 (1) (2022), 15459.

[25] L.W. von Friesen, et al., An efficient and gentle enzymatic digestion protocol for the extraction of microplastics from bivalve tissue, Mar. Pollut. Bull. 142 (2019) 129–134.

[26] K. Enders, et al., Extraction of microplastic from biota: recommended acidic digestion destroys common plastic polymers, ICES J. Mar. Sci. 74 (1) (2017) 326–331.

[27] A. Gondikas, K. Mattsson, M. Hassellöv, Methods for the detection and characterization of boat paint microplastics in the marine environment, Frontiers in Environmental Chemistry 4 (2023).

[28] J. Strand, Z. Tairova, Microplastics Particles in North Sea Sediments 2015, Scientific Report from DCE- Danish Center for Environment and Energy, 2016. **No. 178**.